Title
Discriminating symbiosis and immunity signals by receptor competition in rice

Journal
Proceedings of the National Academy of Sciences of the United States of America, 118(16)

ISSN
0027-8424

Authors
Zhang, Chi
He, Jiangman
Dai, Huiling
et al.

Publication Date
2021-04-20

DOI
10.1073/pnas.2023738118

Peer reviewed

Discriminating symbiosis and immunity signals by receptor competition in rice

Chi Zhang (张弛)[a,b,1], Jiangman He[a,b,1], Huiling Dai[a], Gang Wang[a], Xiaowei Zhang[a], Chao Wang[a], Jincai Shi[a,b], Xi Chen[a,b], Dapeng Wang[c], and Ertao Wang[a,2]

[a]National Key Laboratory of Plant Molecular Genetics, Chinese Academy of Sciences Center for Excellence in Molecular Plant Sciences, Institute of Plant Physiology and Ecology, Shanghai Institutes for Biological Sciences, Chinese Academy of Sciences, 200032 Shanghai, China; [b]University of the Chinese Academy of Sciences, 100039 Beijing, China; and [c]State Key Laboratory of Agrobiotechnology, College of Biological Sciences, China Agricultural University, 100193 Beijing, China

Edited by Éva Kondorosi, Hungarian Academy of Sciences, Biological Research Centre, Szeged, Hungary, and approved March 10, 2021 (received for review November 30, 2020)

Plants encounter various microbes in nature and must respond appropriately to symbiotic or pathogenic ones. In rice, the receptor-like kinase OsCERK1 is involved in recognizing both symbiotic and immune signals. However, how these opposing signals are discerned via OsCERK1 remains unknown. Here, we found that receptor competition enables the discrimination of symbiosis and immunity signals in rice. On the one hand, the symbiotic receptor OsMYR1 and its short-length chitooligosaccharide ligand inhibit complex formation between OsCERK1 and OsCEBiP and suppress OsCERK1 phosphorylating the downstream substrate OsGEF1, which reduces the sensitivity of rice to microbe-associated molecular patterns. Indeed, OsMYR1 overexpression lines are more susceptible to the fungal pathogen *Magnaporthe oryzae*, whereas *Osmyr1* mutants show higher resistance. On the other hand, OsCEBiP can bind OsCERK1 and thus block OsMYR1–OsCERK1 heteromer formation. Consistently, the *Oscebip* mutant displayed a higher rate of mycorrhizal colonization at early stages of infection. Our results indicate that OsMYR1 and OsCEBiP receptors compete for OsCERK1 to determine the outcome of symbiosis and immunity signals.

rice | arbuscule mycorrhizal symbiosis | receptors | competition | immunity

In nature, plants live and interact with diverse microbes, including symbionts and pathogens. To discern friends from foes, plants have evolved various receptors that sense external microbes. Plant immune responses are triggered when pattern recognition receptors (PRRs) at the plasma membrane recognize microbe-associated molecular patterns (MAMPs) (1). MAMPs are highly conserved molecular signatures within a class of microbes and include fungal chitin, bacterial flagellin, and elongation factor Tu (EF-Tu) (2). PRRs comprise receptor-like kinases and receptor-like proteins (3). In plant–symbiont interactions, receptor kinases at the plasma membrane recognize signals that trigger symbiosis (4, 5).

Arbuscular mycorrhizal (AM) fungi secrete short-chain chitooligosaccharides (COs) and nonsulfated lipochitooligosaccharides (LCOs), called mycorrhizal factors (Myc factors), that are recognized by plant receptors and mediate the establishment of AM symbiosis (6–14). In rice, perception of the AM symbiotic signal is mediated by a lysin motif (LysM)–containing receptor kinase (LYKs), OsMYR1, that directly binds to CO4 and subsequently interacts with OsCERK1 (8). Interestingly, OsCERK1 is also a well-known receptor involved in MAMP-triggered immunity (15–17). In rice, an OsCERK1–OsCEBiP receptor complex recognizes chitin and triggers immune responses (18). Additionally, OsCERK1 interacts with OsLYP4 and OsLYP6 to participate in peptidoglycan perception (19). Thus, OsCERK1 is a node that crosses immunity and symbiosis.

Fungal cell walls consist of about 1 to 20% chitin, which is a long-chain polymer of N-acetylglucosamine. To protect themselves from fungal infection, plants secrete chitinases that break down chitin and release COs (20). Long-chain COs are recognized by specific receptors and trigger immunity, whereas short-chain COs are associated with non-stress–related plant responses (21). Similarly, in mammals, shorter oligomers induce a weaker defense response than longer oligomers (22). Intriguingly, although chitin is the principal component of AM fungi, AM symbiosis triggers only a weak defense response (23, 24). Moreover, pretreatment of plants with CO4 also suppresses their defense response (21), implying that CO4 and OsMYR1 might suppress defense responses during AM symbiosis. However, the mechanism remains unclear.

Interestingly, a recent study reported that COs ranging from four to eight residues in length (CO4 to CO8) can serve as symbiotic signals in *Medicago truncatula*, although CO8 is typically considered an immunity signal (9, 25). In rice, LCOs cannot induce symbiotic calcium oscillations, and short-chain COs are the major symbiotic signals from mycorrhizal fungi (26). In this study, we found that the shorter-chain chitooligosaccharide CO4 and its receptor OsMYR1 can suppress immune signaling induced by CO8 in rice. Our data indicate that the balanced perception of CO4 and CO8 by the symbiotic receptor OsMYR1, and the MAMP receptor OsCEBiP is crucial for the establishment of AM symbiosis in rice.

PLANT BIOLOGY

Results

CO8 Activates Both Immunity and Symbiotic Signaling but Inhibits AM Symbiosis in Rice. Like other fungi, AM fungal cell walls also contains chitin. Therefore, we assayed whether AM fungi could

Significance

Plant adaptation in nature relies on the appropriate response to symbiotic and pathogenic microbes. Chitin is an important component of the mycorrhizal fungi cell wall and a major microbe-associated molecular pattern (MAMP), which can activate pattern recognition receptors and trigger plant immunity. How MAMP-triggered immunity is suppressed by symbiotic fungi to establish symbiosis remains elusive. Here, we found that the CO4 (Chitotetraose) symbiotic receptor OsMYR1 cannot only initiate symbiotic signaling but also can repress rice immunity by depleting the receptor-like kinase OsCERK1, thereby preventing the formation of the immunity complex OsCERK1–OsCEBiP. We propose that receptor competition for OsCERK1 in rice underlies a switch that discerns defense and symbiotic signals.

Author contributions: C.Z., J.H., and E.W. designed research; C.Z., J.H., H.D., G.W., X.Z., C.W., J.S., and X.C. performed research; C.Z., J.H., G.W., X.Z., D.W., and E.W. analyzed data; and C.Z., J.H., and E.W. wrote the paper.

The authors declare no competing interest.

This article is a PNAS Direct Submission.

See online for related content such as Commentaries.

[1]C.Z. and J.H. contributed equally to this work.

[2]To whom correspondence may be addressed. Email: etwang@cemps.ac.cn.

This article contains supporting information online at https://www.pnas.org/lookup/suppl/doi:10.1073/pnas.2023738118/-/DCSupplemental.

Published April 14, 2021.

trigger MAMP-triggered immunity in rice. Briefly, stems and roots of wild-type (WT) rice were treated with germinated spore exudates (GSE) for 10 min, and the activation of MAPKs (Mitogen-Activated Protein Kinases) was measured as a reporter of the defense response (6). We observed strong activation of MAPKs by GSEs from the pathogenic fungus *Magnaporthe oryzae* and from the AM fungi *Rhizophagus irregularis* (*SI Appendix*, Fig. S1). Moreover, treatment with purified CO8 triggered MAPK activation and ROS (reactive oxygen species) production in rice roots (Fig. 1 *A* and *B* and *SI Appendix*, Fig. S1). Intriguingly, CO8 treatment also triggered symbiotic calcium oscillations in rice root epidermal cells (Fig. 1*C*), which is consistent with recent observations in *Medicago* (9).

Our data reveal that CO8 can activate opposite responses in plant immunity and symbiosis. To investigate the role of CO8 in mycorrhizal symbiosis, we assayed whether CO8 treatment affects mycorrhizal colonization in rice. We observed reduced colonization of AM fungi in CO8-treated roots compared to controls (Fig. 1*D*). Thus, we conclude that CO8 can induce both symbiotic and immunity signals, but, overall, CO8 as a MAMP inhibits mycorrhizal colonization in rice.

CO4 Promotes Symbiosis and Suppresses Immunity via *OsMYR1*. CO4 is the key signal molecule for AM symbiosis in rice (8), and we found that CO4 treatment promotes mycorrhizal colonization of rice roots (Fig. 2*A*), which is consistent with recent findings in *M. truncatula* (27). We previously showed that OsMYR1 can bind CO4 and is required for mycorrhizal symbiosis (8), and we hypothesized that CO4-promoted mycorrhizal colonization of rice is dependent on *OsMYR1*. To test this hypothesis, we inoculated *Osmyr1-1*, *Osmyr1-2* mutants, and WT roots with mycorrhizal fungi and quantified AM colonization at 5 wk postinoculation (wpi). Indeed, we found that CO4-promoted mycorrhizal infection is dependent on *OsMYR1* (Fig. 2*A*), suggesting that CO4 must be perceived by OsMYR1 to promote mycorrhizal colonization.

Pretreatment of plants with either CO4 or Nod factor can suppress the immunity response induced by bacterial flagellin-flg22 (21). To investigate whether CO4 can suppress CO8-triggered immune responses, we treated rice with CO4 and/or CO8 and measured MAPK activation and ROS production. CO4 treatment alone slightly activated MAPKs but not as efficiently as CO8 (*SI Appendix*, Fig. S2*A*). CO4 pretreatment did not suppress CO8-induced activation of MAPKs (*SI Appendix*, Fig. S2*A*), but it did reduce CO8-induced ROS production (Fig. 2*B*).

We further assessed the role of the CO4 receptor *OsMYR1* in the suppression of immunity. We found that CO8-induced MAPK activation and ROS production are stronger in *Osmyr1* mutant roots compared to WT roots (Fig. 2 *C* and *D*). Moreover, CO4 pretreatment did not inhibit CO8-induced ROS production in *Osmyr1* mutants (Fig. 2*D*).

Together, these data indicate that CO4 is not only a signal molecule to promote AM symbiosis but also serves to partly suppress immunity and CO8 signaling, through its receptor OsMYR1.

OsMYR1 Depletes OsCERK1, Inhibiting Its Homodimerization and Interaction with OsCEBiP. OsCERK1 and OsCEBiP were reported to associate in an immunity receptor complex mediating chitin perception (17). We investigated how CO4 affects the OsCERK1–OsCEBiP interaction and found that CO4 treatment reduced the coimmunoprecipitation of OsCERK1-HA (OsCERK1 fused to a C-terminal Hemagglutinin tag) with OsCEBiP-FLAG (OsCEBiP fused to a C-terminal DYKDDDDK peptide tag) in *Arabidopsis* protoplasts (Fig. 3*A*). These data suggest that CO4 suppresses immunity by inhibiting formation of the immunity receptor complex.

We hypothesized that the CO4 receptor OsMYR1 represses CO8 signaling by inhibiting the OsCERK1–OsCEBiP interaction. To test this hypothesis, we transiently coexpressed OsMYR1-GFP (OsMYR1 fused to a C-terminal green fluorescent protein tag), OsCERK1-HA, and OsCEBiP-FLAG in *Atcerk1 Arabidopsis* protoplasts. We found that OsCERK1-HA coimmunoprecipitated with OsCEBiP-FLAG, as expected, but this interaction was weakened upon coexpression of OsMYR1-GFP; what's more, exogenous application of CO4 further weakened the interaction between

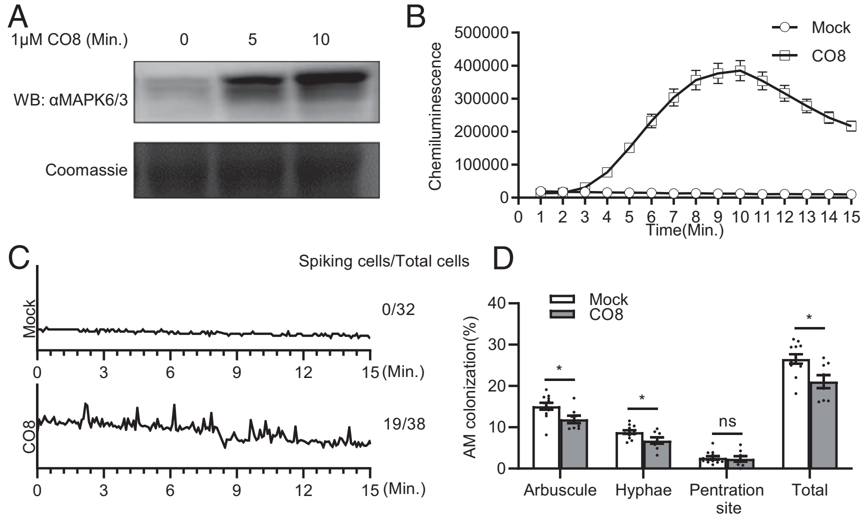

Fig. 1. CO8 activates both immunity and symbiotic signals but inhibits symbiosis. (*A*) CO8-induced MAPK activation in the roots of 7-d-old seedlings of Nipponbare. Roots were treated with 1 μM CO8. Samples were collected at 0, 5, and 10 min and analyzed by immunoblotting using anti–p44/42-ERK antibody. Coomassie brilliant blue staining is shown as a loading control. The experiments were repeated three times with similar results. (*B*) ROS production in the roots of 7-d-old seedlings of Nipponbare treated with 1 μM CO8. ROS were detected with a luminol–chemiluminescence assay. Error bars represent SE ($n = 12$). (*C*) Representative calcium response in rice atrichoblasts (root epidermal cells) treated with 100 nM CO8 in 7-d-old seedlings of Nipponbare stably transformed with a nuclear-localized YC3.6. The number of cells showing calcium oscillations is indicated relative to the total cells analyzed. (*D*) AM colonization of Nipponbare. Rice was inoculated with *R. irregularis* for 5 wk and treated with H_2O or 1 μM CO8 when watering. AM colonization in roots was examined by staining with ink-acetic acid. Error bars represent SE ($n = 12$). Statistical significance for each fungal structure between Mock and CO8 treatment groups were assessed by Student's t test ($P < 0.05$). This is a representative experiment that was repeated three times with similar results. ''Total'' means the sum of all fungal structures including arbuscule, internal hyphae, and penetration sites.

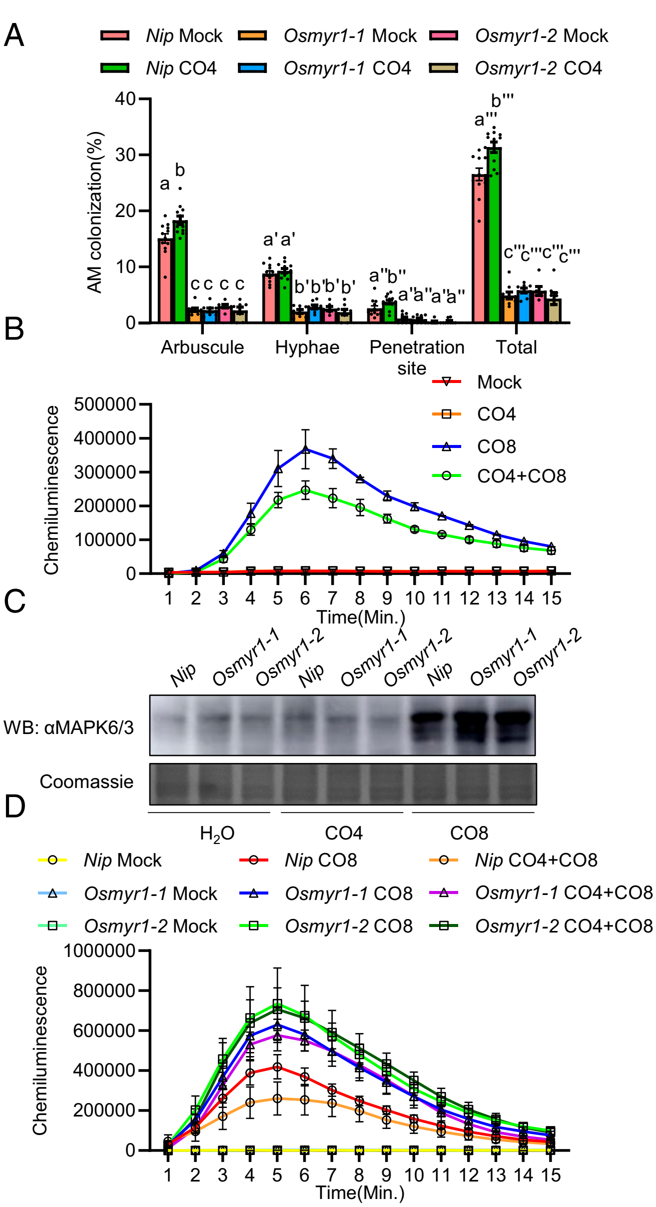

Fig. 2. CO4-promoted symbiosis and CO4-suppressed immunity required *OsMYR1*. (*A*) AM colonization of *Osmyr1-1*, *Osmyr1-2*, and Nipponbare. Rice was inoculated with *R. irregularis* for 5 wk and treated with H_2O or 1 μM CO4 when watering. AM colonization in roots was examined by staining with ink-acetic acid. Error bars represent SE (n = 12). Statistical significance for each fungal structure between WT and mutants with Mock and CO4 treatment groups were assessed by two-way ANOVA (P < 0.05). This is a representative experiment that was repeated three times with similar results. "Total" means the sum of all fungal structures including arbuscule, internal hyphae, and penetration sites. (*B*) CO4 suppresses the production of ROS induced by CO8. A total of 2 cm root tips from 10-d-old rice were treated with 1 μM CO4 or 1 μM CO8 or pretreated with 1 μM CO4 for 30 min then treated with 1 μM CO8 for 10 min. ROS were detected with a luminol–chemiluminescence assay. Error bars represent the SE (n = 6). (*C*) Activation of MAPKs in the roots of *Osmyr1-1*, *Osmyr1-2*, and WT. Roots were treated with water, 1 μM CO4, or 1 μM CO8 for 10 min and analyzed by immunoblotting using anti–p44/42-ERK antibody. Coomassie staining is shown as a loading control. The experiments were repeated three times with similar results. (*D*) Production of CO8-induced ROS burst in *Osmyr1-1* and *Osmyr1-2* are higher than WT and cannot be inhibited by CO4 pretreatment. A total of 2 cm of root tips from 10-d-old rice were treated with 1μM CO8 or pretreated with 1μM CO4 for 30 min then treated with 1 μM CO8 for 10 min. ROS were detected with a luminol–chemiluminescence assay. Error bars represent the SE (n = 10).

OsCEBiP-FLAG and OsCERK1-HA (Fig. 3*B* and *SI Appendix*, Fig. S2*B*). These data suggest that OsMYR1 can interfere with the OsCERK1–OsCEBiP interaction to inhibit plant immunity in rice, and CO4 can enhance this inhibition.

In *Arabidopsis*, AtCERK1 dimerization is critical for chitin-triggered immunity (25). To assess the dimerization of OsCERK1, we purified the OsCERK1 kinase domain ($OsCERK1^{KD}$) fused to MBP (maltose binding protein tag) or His (polyhistidine tag). We found that MBP-$OsCERK1^{KD}$ interacted with His-$OsCERK1^{KD}$ in an in vitro pull-down assay (*SI Appendix*, Fig. S2*C*), consistent with dimerization. Importantly, the His-$OsMYR1^{KD}$ and MBP-$OsCERK1^{KD}$ interaction was more robust than $OsCERK1^{KD}$ homodimer, and $OsCERK1^{KD}$ dimerization was completely blocked by $OsMYR1^{KD}$ (*SI Appendix*, Fig. S2*C*). We subsequently investigated how OsMYR1 affects OsCERK1 homodimerization in vivo. OsCERK1-FLAG interacted with OsCERK1-HA in *Arabidopsis* protoplasts (*SI Appendix*, Fig. S2*D*). Again, OsMYR1-GFP inhibited formation of the homodimer and weakly interacted with OsCERK1-FLAG in *Arabidopsis* protoplasts (*SI Appendix*, Fig. S2*D*). These data suggest that OsMYR1 binds to OsCERK1, thereby reducing its homodimerization and its interaction with OsCEBiP and thus suppressing plant immunity in rice.

OsMYR1 Suppresses OsCERK1-Mediated Phosphorylation of Its Substrates In Vitro. The OsCERK1 kinase phosphorylates several substrates, including OsGEF1, OsRLCK185, and OsMYR1 (28, 29). To further examine how OsMYR1 affects OsCERK1, we evaluated the kinase activity of OsCERK1 in vitro. We found that MBP-$OsCERK1^{KD}$ phosphorylated itself and GST-OsGEF1 (OsGEF1 fused N-terminally to glutathione S-transferase tag), while GST-$OsMYR1^{KD}$ inhibited these reactions in a dose-dependent manner (Fig. 3*C*). MBP-$OsCERK1^{KD}$ efficiently phosphorylated GST-$OsMYR1^{KD}$ (Fig. 3*C*). In contrast, GST-$OsMYR1^{KD}$ did not inhibit the MBP-$OsCERK1^{KD}$–mediated phosphorylation of His-OsRLCK185-K108E (kinase-inactive mutant) (*SI Appendix*, Fig. S2*E*). We speculate that OsCERK1 has a higher affinity for OsRLCK185 than for OsGEF1. These data suggest that OsMYR1 attenuates defense signaling by inhibiting OsCERK1-mediated phosphorylation of its substrates.

***OsMYR1* Inhibits Plant Immunity in Rice Roots.** Given our findings that OsMYR1 and its ligand CO4 can inhibit the interaction between OsCERK1 and OsCEBiP, we investigated how OsMYR1 affects plant immunity. Briefly, we established a system whereby *M. oryzae* can invade plants from the roots (30–32) and measured lesion length in the roots of WT and *Osmyr1* mutant plants. We observed pathogen-induced browning in the root at 2 wpi (Fig. 3*D*). Importantly, the lesion length was shorter in *Osmyr1* mutant roots compared to WT roots (Fig. 3*E*). We also inoculated the leaves of WT and *Osmyr1* mutant with *M. oryzae* but did not observe a difference in lesion areas (*SI Appendix*, Fig. S3). This finding is consistent with our previous study showing that *OsMYR1* is expressed in roots (8). Moreover, our qRT-PCR analysis revealed that *OsMYR1* is dramatically induced by *R. irregularis* inoculation in roots but not in stems or leaves (*SI Appendix*, Fig. S4). We stained the fungi in roots with wheat germ agglutinin (WGA) and observed dense hyphae with similar morphology in the lesion area of WT and *Osmyr1* mutants (*SI Appendix*, Fig. S5 *A*–*D*). However, the relative fungal growth biomass which reflects the amount of fungus on the roots was lower in *Osmyr1* mutant root compared to WT root (*SI Appendix*, Fig. S5*E*), as revealed by the ratio of expression of *M. oryzae Pot2* versus rice *ubiquitin* (33).

To determine whether *OsMYR1* negatively regulates defense-related genes during *M. oryzae* infection, we analyzed the expression of the immunity markers *OsPR10*, *OsPBZ1*, and *OsCHITINASE*. Our qRT-PCR analysis showed that the three marker genes were more highly expressed in infected *Osmyr1* mutants compared to infected WT plants (*SI Appendix*, Fig. S5*F*). In summary, in the

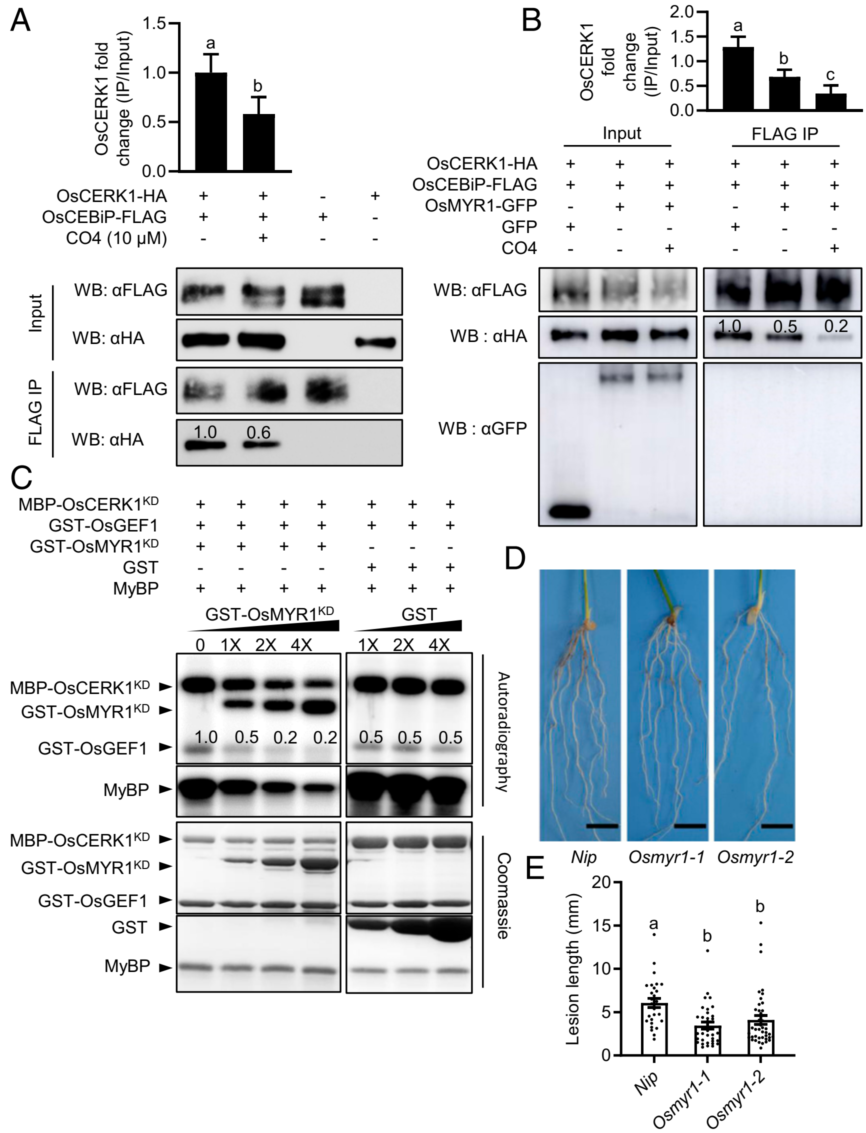

Fig. 3. OsMYR1 depletes OsCERK1 for OsCERK1–CEBiP formation and inhibits immunity. (*A*) CO4 treatment of *Arabidopsis* protoplasts suppresses OsCERK1-HA and OsCEBiP-FLAG complex formation. OsCERK1-HA and OsCEBiP-FLAG were transiently coexpressed in protoplasts. OsCERK1-HA and OsCEBiP-FLAG were detected by immunoblot analysis with anti-HA or anti-FLAG antibody, respectively, after immunoprecipitation with anti-FLAG antibody. Letters indicate significant difference assessed by one-way ANOVA, $P < 0.05$. (*B*) OsMYR1-GFP and CO4 inhibit the interaction of OsCEBiP-FLAG and OsCERK1-HA in *Atcerk1 Arabidopsis* protoplasts. OsMYR1-GFP or GFP were transiently expressed in protoplast with OsCEBiP-FLAG and OsCERK1-HA. OsCERK1-HA, OsCEBiP-FLAG, and OsMYR1-GFP were detected by immunoblot analysis with anti-HA, anti-FLAG, and anti-GFP antibody, respectively, after immunoprecipitation with anti-FLAG antibody. Letters indicate significant difference assessed by one-way ANOVA, $P < 0.05$. (*C*) GST-OsMYR1^{KD} attenuates MBP-OsCERK1^{KD}-mediated phosphorylation of GST-OsGEF1 in vitro. The in vitro phosphorylation reaction was performed using proteins purified from *Escherichia coli* and [γ-^{32}P] ATP, and detected by autoradiography. Coomassie-stained gel shows the positions of substrate proteins. (*D*) Weaker infection of rice blast (virulent isolate TH12) fungal pathogen in *Osmyr1-1* and *Osmyr1-2* roots than in WT roots. Lesions were photographed at 2 wpi. The experiment was repeated three times and showed the same result. (Scale bar, 10 mm.) (*E*) Disease resistance to rice blast in the *Osmyr1-1*, *Osmyr1-2*, and WT, measured by lesion length. Error bars denote SE (n = 41). Letters indicate significant difference assessed by one-way ANOVA, $P < 0.05$. This is a representative experiment that was repeated three times with similar results. Numbers above western and autoradiography bands represent the relative signal intensity detected by using ImageJ software. The histogram above shows a statistical analysis of the relative signal intensity based on three repeated experiments.

Osmyr1 mutant, defense-related signaling is enhanced, and the invasion of rice blast is suppressed. So, the length of lesions caused by fungal growth is shorter in *Osmyr1*. Altogether, our data suggest that *OsMYR1* suppresses MAMP-triggered immunity, which is important for rice responses to fungal pathogens.

Overexpression of *OsMYR1* Suppresses Plant Immunity in Rice Roots. To further investigate the negative regulation of plant immunity by *OsMYR1*, we overexpressed *OsMYR1-GFP* (*OE-OsMYR1*) and examined the early MAMP-triggered immunity response in roots. Unexpectedly, CO8-induced ROS production was enhanced in two *OE-OsMYR1* transformed lines (*OsMYR1-GFP-9* and *OsMYR1-GFP-13*) compared to WT (*SI Appendix*, Fig. S6*A*). Previously, we showed that OsMYR1 can also bind CO8, suggesting that OsMYR1 might induce ROS production upon binding CO8 (8). However, a 30-min pretreatment with CO4 completely suppressed CO8-activated ROS production in *OE-OsMYR1* lines (*SI Appendix*, Fig. S6*A*). Moreover, CO8-mediated activation of MAPKs was comparable between *OE-OsMYR1* lines and WT (*SI Appendix*, Fig. S6*B*). Intriguingly, a 30-min pretreatment of CO4 significantly reduced CO8-activated MAPKs in *OE-OsMYR1* lines (*SI Appendix*, Fig. S6*B*), suggesting that overexpression of *OsMYR1* can stimulate CO4-mediated suppression of CO8-mediated MAPK activation.

Additionally, we inoculated the roots of *OE-OsMYR1* plants with *M. oryzae*. *OE-OsMYR1* plants showed no apparent growth phenotype (*SI Appendix*, Fig. S7). However, *M. oryzae* invasion significantly suppressed root growth in *OE-OsMYR1* plants compared to WT plants (Fig. 4*A*), indicating that *OE-OsMYR1* is more susceptible to fungal pathogen infection. Further quantification of the fungal lesion length and biomass showed increased invasion of *M. oryzae* in the roots of *OE-OsMYR1* compared to WT rice (Fig. 4 *B*–*D*). Consistent with these data, defense-related marker genes displayed lower expression in infected *OE-OsMYR1* lines compared to infected WT (Fig. 4*E*). Altogether, our data suggest *OsMYR1* negatively regulates plant immunity and enhances susceptibility to fungal pathogen infection.

OsCEBiP Negatively Regulates AM Symbiosis. The OsCERK1–OsMYR1 receptor complex is required for AM symbiosis, whereas the OsCERK1–OsCEBiP is required for chitin-triggered immunity. We showed that OsMYR1 can interfere with OsCERK1–OsCEBiP-mediated immunity (Fig. 3) and that OsMYR1-GFP interacts with OsCERK1-HA (Fig. 5*A*) in *Arabidopsis* protoplasts. Intriguingly, expression of OsCEBiP-FLAG inhibited the interaction between OsMYR1-GFP and OsCERK1-HA in a CO8-dependent manner (Fig. 5*A*), suggesting that the MAMP receptor OsCEBiP might in turn affect AM symbiosis process.

A previous study showed that an *Oscebip* mutant had a comparable AM phenotype to WT at 5 wpi with a high concentration

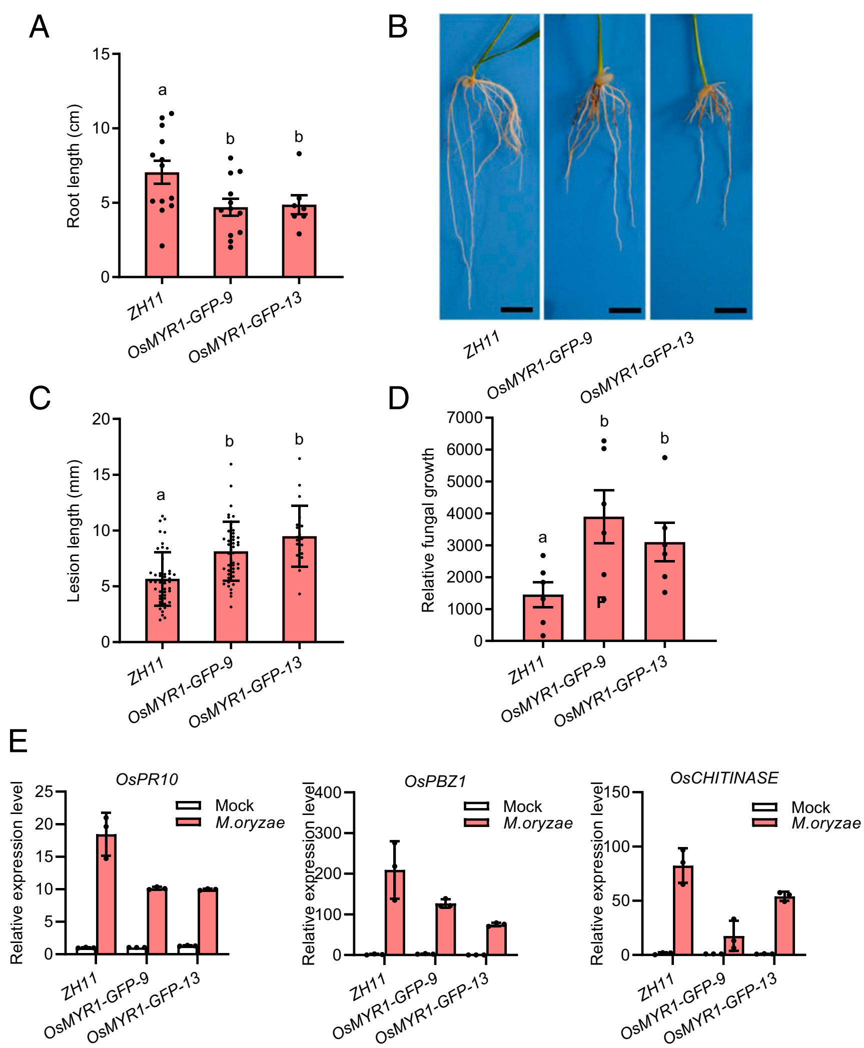

Fig. 4. Overexpression of OsMYR1-GFP decreases plant resistance to rice blast in root. (*A*) Root length of *OsMYR1-GFP-9*, *OsMYR1-GFP-13*, and WT at 2 wpi. Error bars denote SE (n = 13). Letters indicate significant difference assessed by one-way ANOVA, $P < 0.05$. This is a representative experiment that was repeated three times with similar results. (*B*) Infection of rice blast fungal pathogen in *OsMYR1-GFP-9* and *OsMYR1-GFP-13* roots are weaker than that in WT. Lesions were photographed at 2 wpi. The experiment was repeated three times and showed the same result. (Scale bar, 10 mm.) (*C*) Disease resistance to rice blast in the *OsMYR1-GFP-9*, *OsMYR1-GFP-13*, and WT, measured by lesion length. Error bars denote SE (n = 46). Letters indicate significant difference assessed by one-way ANOVA, $P < 0.05$. This is a representative experiment that was repeated three times with similar results. (*D*) Disease resistance to rice blast in the *OsMYR1-GFP-9*, *OsMYR1-GFP-13*, and WT, measured by relative fungal growth. Error bars denote SE (n = 6). Letters indicate significant difference assessed by one-way ANOVA, $P < 0.05$. This is a representative experiment that was repeated three times with similar results. (*E*) Relative expressions of defense-related marker genes *OsPR10*, *OsPBZ1*, and *OsCHITINASE* in *OsMYR1-GFP-9*, *OsMYR1-GFP-13*, and WT roots at 2 wpi by real-time PCR. Error bars indicate SD of three technical repeats. This is a representative experiment that was repeated three times with similar results.

of *R. irregularis* (5,000 spores per plant) (15). We employed a lower concentration of spores (400 spores per plant) and similarly did not observe differences in colonization between *Oscebip* mutant and WT at 3 or 4 wpi (*SI Appendix*, Fig. S8 *A* and *B*). Intriguingly, we did observe higher mycorrhizal infections in the *Oscebip* mutant compared to WT at 2 wpi (Fig. 5*B*). Considering that the chitin from *R. irregularis* cell wall induces a defense response, we infer that at the early stage of AM symbiosis, chitin can induce plant immunity through the OsCEBiP–OsCERK1 receptor, which would have a negative effect on mycorrhizal fungal infection. Consistent with this inference, the relative transcript levels of the immunity markers *OsPBZ1*, *OsCHITINASE*, and *OsPR10* are lower in the *R. irregularis*–inoculated *Oscebip* mutant versus WT (Fig. 5*C*), suggesting that the MAMP receptor OsCEBiP negatively regulates AM symbiosis at the early stage of infection.

Discussion

In nature, plants interact constantly with microbes and must respond appropriately to symbiotic versus pathogenic microbes in order to survive (34). Chitin is a major component of the cell wall in both symbiotic and pathogenic fungi and acts as a MAMP to trigger plant immunity (35, 36). AM fungi can establish a symbiotic association with plants without inducing an intense defense response; however, a weak plant immunity response is always observed (23, 24). The weak defense response triggered by MAMPs of symbiotic fungi might be important to regulate the expression of immunity-related genes and enhance resistance to pathogens (23, 37).

In this study, we show that CO4 secreted from AM fungi can suppress MAMP-triggered immunity in rice, similar to Nod factor-mediated inhibition of the flg22-induced immune response (21). OsMYR1 can partially diminish the defense response, in addition to its function in perceiving Myc factor during AM symbiosis. Therefore, OsMYR1 not only serves as a receptor of the Myc signal but also as an inhibitor to suppress plant immunity. The CO8-triggered defense signal and CO4-induced symbiosis signal both required the kinase OsCERK1 to phosphorylate specific substrates and trigger downstream events. The receptors involved in defense (OsCEBiP) and symbiosis (OsMYR1) compete for the coreceptor OsCERK1 (Fig. 5*D*). We further show that the discrimination of symbiosis and immunity signals by interreceptor complex competition plays a key role in the early stage of mycorrhizal fungal infection in rice. Thus, we propose that OsCERK1 functions as a common receptor for both defense and symbiosis signaling that can trigger either of two opposing signal outputs depending on the context.

AM symbiosis appears to be established at the cost of plant immunity; plants must limit defense responses from some tissues to promote symbiosis and yet maintain immunity in other tissues. In the legume–rhizobial symbiosis, nodules display a weak defense response upon pathogen infection, but in *M. truncatula*, this weakened defense response is limited to nodules (38), indicating a spatiotemporal suppression of MAMP-triggered immunity during symbiosis. In addition, it is known that pathogens can secrete different types of effectors to interfere with plant immunity (39, 40). Similarly, symbiotic rhizobia and AM fungi can also secrete effectors to suppress plant defense response and promote symbiosis (41–43). It will be important to investigate how plants maintain the immunity response in a spatiotemporal-specific manner, while employing different strategies for plant–microbe symbioses.

Materials and Methods

Coimmunoprecipitation Assays. Coding regions of *OsCERK1*, *OsCEBiP*, and *OsMYR1* were inserted into modified plasmids pUC19-HA (hemagglutinin tag), pUC19-FLAG (DYKDDDDK peptide tag), and/or pUC19-GFP (green fluorescent protein tag), respectively. After protoplast transformation, total protein was extracted with extraction buffer containing 50 mM Tris–HCl (pH 7.5), 150 mM NaCl, 10% glycerol, 1% Triton X-100, and 1 × EDTA (ethylenediaminetetraacetic acid)-free protease inhibitor mixture (Roche) from 5×10^6 protoplasts expressing OsCERK1-HA, OsCEBiP-FLAG/-HA, and OsMYR1-FLAG/-GFP. The extracted proteins were incubated with prewashed anti-FLAG M2 agarose beads (Sigma-Aldrich) for 2 h at 4 °C. After washing three times with extraction buffer, the beads were boiled with 1 × sodium dodecyl sulfate loading buffer and loaded for Western blot detection by using anti-FLAG, anti-HA, and anti-GFP antibodies (Sigma-Aldrich). To analyze whether CO4 (Chitotetraose) or CO8 (Chitotetraose) has an effect on the interaction of OsCERK1–OsCEBiP or OsCERK1–OsMYR1, we treated transformed protoplasts with either H_2O or 10 μM CO4 or CO8 (IsoSep) for 10 min before protein extraction.

Pull-Down Assay. Supernatants containing MBP–OsCERK1^{KD} fusion protein were incubated with MBP beads for 3 h at 4 °C. After washing five times with column buffer containing 20 mM Tris–HCl (pH 7.4), 200 mM NaCl, 10 mM EDTA, 1 mM dithiothreitol (DTT), and protease inhibitor mixture (Roche), the beads were incubated with affinity-purified His-OsCERK1^{KD} and with or without affinity-purified His-OsMYR1^{KD} for 3 h. Finally, the beads were collected and washed five times with RIPA buffer (radioimmunoprecipitation assay buffer) (500 mM NaCl, 20 mM Tris–HCl [pH 8.0], 1 mM DTT, 0.1% Triton X-100, and protease inhibitor mixture) (44). The proteins eluted from beads were then used for Western blot analysis with anti-MBP (Abmart) and anti-His (Cwbio) antibodies.

Phosphorylation Assay. In vitro kinase assays were performed as previously described (28). The kinase reaction was performed at 30 °C for 30 min in a reaction volume of 20 μL containing 50 mM Tris–HCl (pH 7.5), 10 mM $MgCl_2$, 1 mM DTT, 100 mM ATP, 2.5 uCi [γ-^{32}P] ATP, and 3 μg of purified proteins. The reaction was terminated with 1 × loading buffer and subjected to sodium dodecyl sulfate–polyacrylamide gel electrophoresis. Radiolabeled bands were visualized with a Bio-imaging analyzer (BAS-2500) (Fujifilm Life Science).

MAPK Assay. A total 2 cm of roots from root tip of *Oryza sativa* seedlings were cut to 5-mm strips. The roots were floated in water overnight to recover from wounding stress. The materials were then treated with 1×10^{-6} M CO8 (IsoSep) containing 0.1% Silwet L-77 for 10 min followed by freezing in liquid nitrogen. Roots were ground in liquid nitrogen and homogenized in extraction buffer containing 50 mM Tris–HCl (pH 7.5), 150 mM NaCl, 10% glycerol, 1% Triton X-100, 1 × EDTA-free protease inhibitor mixture (Roche), and 1 × PhosSTOP phosphatase inhibitor mixture (Roche). Phosphorylation of MAPK proteins was detected by Western blot with anti–phospho-p44/42 MAPK antibody (Cell Signaling Technology, #4370s).

Measurement of ROS. A total 2 cm of roots from root tip of *O. sativa* seedlings were cut to 5-mm strips. The roots were floated in water overnight to recover from wounding stress. ROS generation after 1×10^{-6} M CO4 or CO8 treatment in the roots strips was monitored using the luminol chemiluminescence assay (33). Four root strips per sample were placed in a well of 96-well plates containing 20 μM of luminol (Wako), 10 μg/mL of horseradish peroxidase (Sigma), and elicitor. Immediately after the treatment, luminescence was measured continuously at 1-min intervals for 15 min with VarioSkan Flash multireader (Thermo Fisher Scientific). In total, 10 replications were performed for each sample and treatment. SEs were calculated for each treatment.

Detection of Calcium Oscillations. For observation of calcium oscillations, nuclear-localized calcium sensor Yellow Cameleon 3.6 (YC3.6) was introduced into Nipponbare (26). To trigger calcium response, we first cultured rice plants axenically on low-nitrogen–buffered nodulation medium plates for 7 d then dissected the apical region (1 to 1.5 cm from the root top) and stuck it to a concave slide for treatment CO8 (IsoSep). Calcium imaging of rice atrichoblasts was performed by using an inverted Zeiss Axio Observer microscope (Zeiss, Germany; https://www.zeiss.com). Calcium sensor YC3.6 was excited by a halogen illuminator through a CFP (cyan fluorescent protein) exciter, and fluorescence emission was captured with a cooled charge coupled device camera after passing through a CFP/yellow fluorescent protein fluorescence resonance energy transfer filter set. Images were acquired every 3 s with 5-ms exposure duration. Ratio of fluorescence intensity in the nucleic region was analyzed using MetaFluor Fluorescence Ratio Imaging Software (Molecular Devices).

Genetic Complementation of *Osmyr1-1*. Cas9-free mutant of *Osmyr1-1* was first identified by using primer pairs Cas9-F and Cas9-R (8). For complementation of *Osmyr1-1* mutant, GFP-tagged *OsMYR1* coding sequence was driven by the *ZmUbiquitin* promoter and expressed in *Osmyr1-1* mutant.

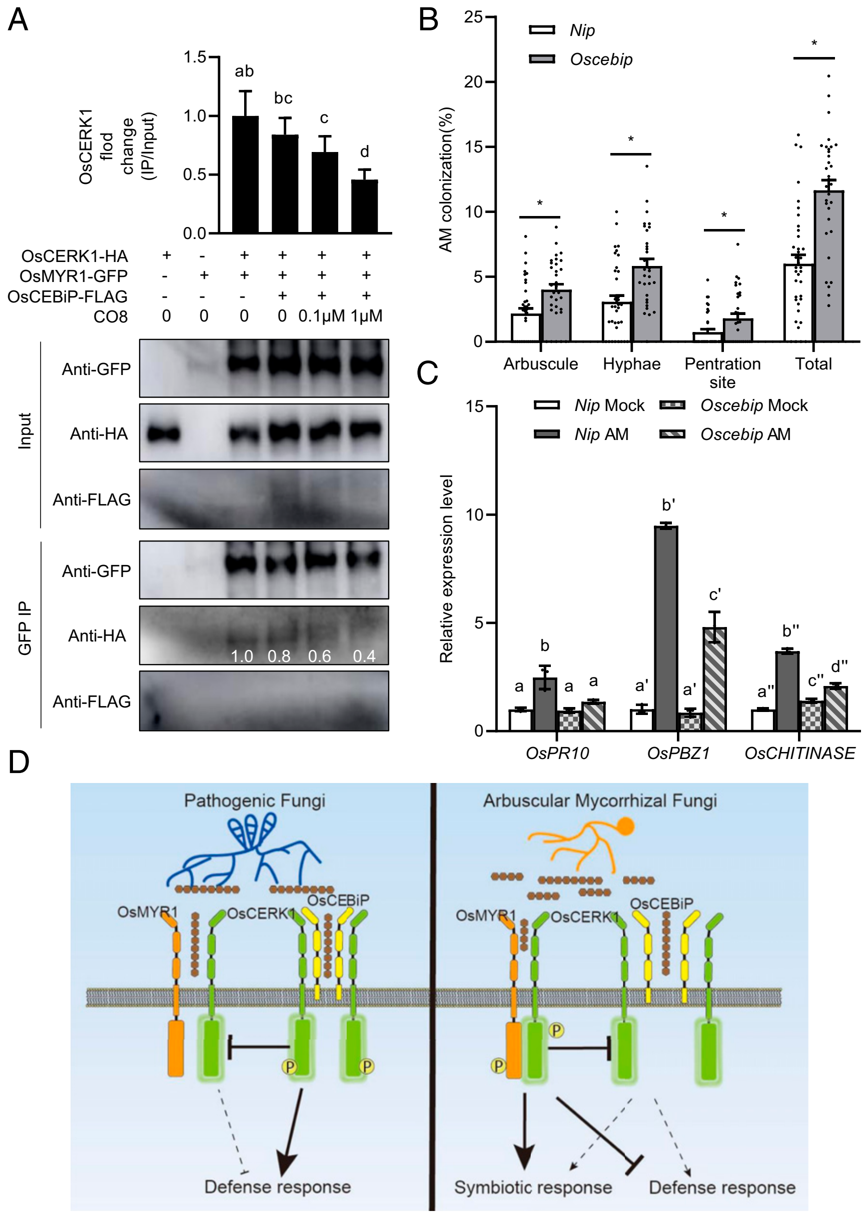

Fig. 5. Receptor competition between OsCEBiP-OsCERK1 and OsMYR1-OsCERK1 balances AM symbiosis and immunity. (*A*) OsCEBiP-FLAG inhibits the interaction of OsMYR1-GFP and OsCERK1-HA in *Arabidopsis* protoplasts. OsCEBiP-FLAG was transiently expressed in protoplasts with OsMYR1-GFP and OsCERK1-HA. OsCERK1-HA, OsCERK1-FLAG, and OsMYR1-GFP were detected by immunoblot analysis with anti-HA, anti-FLAG, and anti-GFP antibody, respectively, after immunoprecipitation with anti-GFP antibody. Letters indicate significant difference assessed by one-way ANOVA, $P < 0.05$. (*B*) AM colonization of *Oscebip* and WT rice. *Oscebip* and WT were inoculated with *R. irregularis* for 2 wk, and AM colonization in roots was examined after staining with ink-acetic acid. Error bars represent SE ($n = 37$). Statistical significance for each fungal structure between *Oscebip* and WT were assessed by Student's *t* test ($P < 0.05$). This is a representative experiment that was repeated three times with similar results. "Total" means the sum of all fungal structures including arbuscule, internal hyphae, and penetration site. (*C*) Relative expressions of defense-related marker genes *OsPR10*, *OsPBZ1*, and *OsCHITINASE* in *Oscebip* and WT roots at 2 wpi by real-time PCR. Error bars indicate SD of three technical repeats. Letters indicate significant difference assessed by one-way ANOVA, $P < 0.05$. This is a representative experiment that was repeated three times with similar results. (*D*) An SPDT (Single Pole Double Throw) switch model in symbiosis and defense signaling pathways. When plants recognize CO8 from fungal pathogen, OsCEBiP will bind OsCERK1 with the help of CO8. This complex formation will inhibit OsMYR1 binding OsCERK1 to activate defense signaling. When plants recognize CO4 from symbiotic fungi, OsMYR1 will bind OsCERK1 with the help of CO4 and inhibit OsCEBiP binding OsCERK1. This complex will activate symbiosis signaling and inhibit defense signaling. OsCERK1 acts as a common receptor that can activate distinct signaling pathways when bound to different coreceptors.

Two independent transgenic lines (*OsMYR1-GFP-9* and *OsMYR1-GFP-13*) were identified using qRT-PCR and Western blot.

Rice Blast Infection Assay. For root infections, roots were infected by *M. oryzae* as described (30). *M. oryzae* cultures for root infection assays were grown on potato dextrose agar for 8 d at 22 °C, and mycelial plugs were taken from the colony margin. The diameter of mycelial plugs is slightly smaller than the tubes to be used later. Fifty-milliliter plastic centrifuge tubes were filled with 35 mL of sterile vermiculite containing 10 mL sterile water. The mycelial plug was placed on top of this and covered with a further 5 mL of vermiculite. Mock-inoculated tubes were placed with sterile agar plugs. Three surface-sterilized seeds were placed on top of the second vermiculite layer, followed by an additional 5 mL of vermiculite and 5 mL of sterile water. Five replicate tubes were set up for each treatment. Tubes were covered with the covers and incubated at 28 °C under 16-h light/8-h dark conditions for 2 to 3 wk. The seedling roots were then washed in water and measured for lesions by a ruler.

For leaf infections, the plantlets were separated with agar and removed to liquid medium in an illumination incubator for about 3 wk until all the plants grew well. For each mutant and WT plant, only the youngest one or two leaves were used for inoculation. Leaves were cut to about 5 cm, placed on two-layer filter paper in a culture vessel, and covered by cotton at both ends. A total 5 mL of sterilized water was added to the filter papers and cotton to maintain high humidity. The spore suspension was added to leaves prewounded by pipet tips. Blast fungus was grown for 2 wk to produce spores. Spores were collected by water and adjusted to 1×10^6 per milliliter. Lengths of lesions were assessed 6 or 7 d after inoculation. A similar method was also used in a previous report (45).

Measurement of Relative Fungal Growth. A total 2 cm infected roots centered on the lesion were cut, and total DNA were extracted using a cetyltrimethylammonium bromide method. The relative expression of *M. oryzae Pot2* gene and the rice *ubiquitin* gene were measured by real-time PCR. The primers sequences of *Pot2* and *ubiquitin* and the computing formula of relative fungal growth are as described (33).

Quantitative RT-PCR Analysis. Total RNA extraction and complementary DNA (cDNA) synthesis were performed as previously described (8). The cDNA was used for quantitative analysis using SYBR Green PCR Mastermix (Genstar) on a CFX96 Touch Real-Time PCR Detection System (Bio-Rad). To measure the expression level of *OsMYR1* and defense-related marker genes, *OsCYCLOPHILIN2* was used as internal control for normalization. Sequences of real-time PCR primers are given in *SI Appendix*, Table S1.

***R. irregularis* Inoculation and CO4 or CO8 Treatment.** Two-week-old rice seedlings were transplanted into a vermiculite and sand (3:1) mixture containing *R. irregularis* spores and cultured in a greenhouse at 28 °C under 16-h light/8-h dark conditions. The spores were produced by an *R. irregularis*/leek coculture and diluted to a final concentration of 400 spores per plant (16).

For CO4 or CO8 treatment during *R. irregularis* inoculation, 4 mL of 1 μM CO4 or CO8 was dropped into each pot with pipette. Treatments were applied weekly, and plants were sampled 5 wpi, after four CO4 or CO8 treatments for morphometric analyses and mycorrhizal intensity determination.

Root Staining. After inoculation with *M. oryzae* for 2 or 3 wk, rice roots were harvested, rinsed, and stained with WGA-Alexa Fluor 488 as previously described (46). *R. irregularis* colonization was stained with ink-acetic acid. Rice roots were soaked in 10% potassium hydroxide for 14 min followed by 6-min staining in ink–vinegar at 95 °C (44). AM colonization was quantified by grid line intersect method (46) and imaged with a Nikon Eclipse 800 light microscope (Nikon).

Data Availability. All study data are included in the article and/or *SI Appendix*.

ACKNOWLEDGMENTS. The research was supported by the NSF (Grants 32088102, 31730103, 31825003 to E.W.), the National Key R&D Program of China (Grants 2019YFA0904703, 2016YFA0500502), the Ministry of Agriculture of China for Transgenic Research (Grants 2016ZX08009-003-001, 2016ZX08009003005-003), and the Strategic Priority Research Program "Molecular Mechanism of Plant Growth and Development" of the Chinese Academy of Sciences (Grant XDB27040207).

1. H. Böhm, I. Albert, L. Fan, A. Reinhard, T. Nürnberger, Immune receptor complexes at the plant cell surface. *Curr. Opin. Plant Biol.* **20**, 47–54 (2014).
2. T. Boller, G. Felix, A renaissance of elicitors: Perception of microbe-associated molecular patterns and danger signals by pattern-recognition receptors. *Annu. Rev. Plant Biol.* **60**, 379–406 (2009).
3. D. Tang, G. Wang, J. M. Zhou, Receptor kinases in plant-pathogen interactions: More than pattern recognition. *Plant Cell* **29**, 618–637 (2017).
4. P. Smit *et al*., *Medicago* LYK3, an entry receptor in rhizobial nodulation factor signaling. *Plant Physiol.* **145**, 183–191 (2007).
5. E. B. Madsen *et al*., A receptor kinase gene of the LysM type is involved in legume perception of rhizobial signals. *Nature* **425**, 637–640 (2003).
6. A. Genre *et al*., Short-chain chitin oligomers from arbuscular mycorrhizal fungi trigger nuclear Ca^{2+} spiking in *Medicago truncatula* roots and their production is enhanced by strigolactone. *New Phytol.* **198**, 190–202 (2013).
7. F. Maillet *et al*., Fungal lipochitooligosaccharide symbiotic signals in arbuscular mycorrhiza. *Nature* **469**, 58–63 (2011).
8. J. He *et al*., A LysM receptor heteromer mediates perception of arbuscular mycorrhizal symbiotic signal in rice. *Mol. Plant* **12**, 1561–1576 (2019).
9. F. Feng *et al*., A combination of chitooligosaccharide and lipochitooligosaccharide recognition promotes arbuscular mycorrhizal associations in *Medicago truncatula*. *Nat. Commun.* **10**, 5047 (2019).
10. C. Gibelin-Viala *et al*., The *Medicago truncatula* LysM receptor-like kinase LYK9 plays a dual role in immunity and the arbuscular mycorrhizal symbiosis. *New Phytol.* **223**, 1516–1529 (2019).
11. D. Liao, X. Sun, N. Wang, F. Song, Y. Liang, Tomato LysM receptor-like kinase SlLYK12 is involved in arbuscular mycorrhizal symbiosis. *Front. Plant Sci.* **9**, 1004 (2018).
12. A. Girardin *et al*., LCO receptors involved in arbuscular mycorrhiza are functional for Rhizobia perception in legumes. *Curr. Biol.* **29**, 4249–4259.e5 (2019).
13. G. Carotenuto *et al*., The rice LysM receptor-like kinase OsCERK1 is required for the perception of short-chain chitin oligomers in arbuscular mycorrhizal signaling. *New Phytol.* **214**, 1440–1446 (2017).
14. Z. Bozsoki *et al*., Receptor-mediated chitin perception in legume roots is functionally separable from Nod factor perception. *Proc. Natl. Acad. Sci. U.S.A.* **114**, E8118–E8127 (2017).
15. K. Miyata *et al*., The bifunctional plant receptor, OsCERK1, regulates both chitin-triggered immunity and arbuscular mycorrhizal symbiosis in rice. *Plant Cell Physiol.* **55**, 1864–1872 (2014).
16. X. Zhang *et al*., The receptor kinase CERK1 has dual functions in symbiosis and immunity signalling. *Plant J.* **81**, 258–267 (2015).
17. T. Shimizu *et al*., Two LysM receptor molecules, CEBiP and OsCERK1, cooperatively regulate chitin elicitor signaling in rice. *Plant J.* **64**, 204–214 (2010).
18. H. Kaku *et al*., Plant cells recognize chitin fragments for defense signaling through a plasma membrane receptor. *Proc. Natl. Acad. Sci. U.S.A.* **103**, 11086–11091 (2006).
19. B. Liu *et al*., Lysin motif-containing proteins LYP4 and LYP6 play dual roles in peptidoglycan and chitin perception in rice innate immunity. *Plant Cell* **24**, 3406–3419 (2012).
20. W. K. Roberts, C. P. Selitrennikoff, Plant and bacterial chitinases differ in antifungal activity. *J. Gen. Microbiol.* **134**, 169–176 (1988).
21. Y. Liang *et al*., Nonlegumes respond to rhizobial Nod factors by suppressing the innate immune response. *Science* **341**, 1384–1387 (2013).
22. K. Fuchs *et al*., The fungal ligand chitin directly binds TLR2 and triggers inflammation dependent on oligomer size. *EMBO Rep.* **19**, e46065 (2018).
23. L. Campos-Soriano, J. García-Martínez, B. San Segundo, The arbuscular mycorrhizal symbiosis promotes the systemic induction of regulatory defence-related genes in rice leaves and confers resistance to pathogen infection. *Mol. Plant Pathol.* **13**, 579–592 (2012).
24. J. Liu *et al*., Arbuscular mycorrhizal symbiosis is accompanied by local and systemic alterations in gene expression and an increase in disease resistance in the shoots. *Plant J.* **50**, 529–544 (2007).
25. T. Liu *et al*., Chitin-induced dimerization activates a plant immune receptor. *Science* **336**, 1160–1164 (2012).
26. J. Sun *et al*., Activation of symbiosis signaling by arbuscular mycorrhizal fungi in legumes and rice. *Plant Cell* **27**, 823–838 (2015).
27. V. Volpe *et al*., Short chain chito-oligosaccharides promote arbuscular mycorrhizal colonization in *Medicago truncatula*. *Carbohydr. Polym.* **229**, 115505 (2020).
28. A. Akamatsu *et al*., An OsCEBiP/OsCERK1-OsRacGEF1-OsRac1 module is an essential early component of chitin-induced rice immunity. *Cell Host Microbe* **13**, 465–476 (2013).
29. C. Wang *et al*., OsCERK1-mediated chitin perception and immune signaling requires receptor-like cytoplasmic kinase 185 to activate an MAPK cascade in rice. *Mol. Plant* **10**, 619–633 (2017).
30. M. Dufresne, A. E. Osbourn, Definition of tissue-specific and general requirements for plant infection in a phytopathogenic fungus. *Mol. Plant Microbe Interact.* **14**, 300–307 (2001).
31. A. Sesma, A. E. Osbourn, The rice leaf blast pathogen undergoes developmental processes typical of root-infecting fungi. *Nature* **431**, 582–586 (2004).
32. S. Marcel, R. Sawers, E. Oakeley, H. Angliker, U. Paszkowski, Tissue-adapted invasion strategies of the rice blast fungus *Magnaporthe oryzae*. *Plant Cell* **22**, 3177–3187 (2010).
33. C. H. Park *et al*., The *Magnaporthe oryzae* effector AvrPiz-t targets the RING E3 ubiquitin ligase APIP6 to suppress pathogen-associated molecular pattern-triggered immunity in rice. *Plant Cell* **24**, 4748–4762 (2012).
34. M. Antolín-Llovera *et al*., Knowing your friends and foes–Plant receptor-like kinases as initiators of symbiosis or defence. *New Phytol.* **204**, 791–802 (2014).
35. T. Shinya, T. Nakagawa, H. Kaku, N. Shibuya, Chitin-mediated plant-fungal interactions: Catching, hiding and handshaking. *Curr. Opin. Plant Biol.* **26**, 64–71 (2015).
36. J. Wan, X. C. Zhang, G. Stacey, Chitin signaling and plant disease resistance. *Plant Signal. Behav.* **3**, 831–833 (2008).
37. Y. Song, D. Chen, K. Lu, Z. Sun, R. Zeng, Enhanced tomato disease resistance primed by arbuscular mycorrhizal fungus. *Front. Plant Sci.* **6**, 786 (2015).
38. C. Benezech *et al*., *Medicago-Sinorhizobium-Ralstonia* co-infection reveals legume nodules as pathogen confined infection sites developing weak defenses. *Curr. Biol.* **30**, 351–358.e4 (2020).
39. L. Lo Presti *et al*., Fungal effectors and plant susceptibility. *Annu. Rev. Plant Biol.* **66**, 513–545 (2015).
40. H. Cui, K. Tsuda, J. E. Parker, Effector-triggered immunity: From pathogen perception to robust defense. *Annu. Rev. Plant Biol.* **66**, 487–511 (2015).
41. D. W. Xin *et al*., Functional analysis of NopM, a novel E3 ubiquitin ligase (NEL) domain effector of Rhizobium sp. strain NGR234. *PLoS Pathog.* **8**, e1002707 (2012).
42. S. Kloppholz, H. Kuhn, N. Requena, A secreted fungal effector of *Glomus intraradices* promotes symbiotic biotrophy. *Curr. Biol.* **21**, 1204–1209 (2011).
43. T. Zeng *et al*., A lysin motif effector subverts chitin-triggered immunity to facilitate arbuscular mycorrhizal symbiosis. *New Phytol.* **225**, 448–460 (2020).
44. N. Yu *et al*., A DELLA protein complex controls the arbuscular mycorrhizal symbiosis in plants. *Cell Res.* **24**, 130–133 (2014).
45. K. Yamaguchi *et al*., A receptor-like cytoplasmic kinase targeted by a plant pathogen effector is directly phosphorylated by the chitin receptor and mediates rice immunity. *Cell Host Microbe* **13**, 347–357 (2013).
46. P. Pimprikar *et al*., A CCaMK-CYCLOPS-DELLA complex activates transcription of RAM1 to regulate arbuscule branching. *Curr. Biol.* **26**, 1126 (2016).